Generating Rational Frames of Space Curves via Hermite Interpolation with Pythagorean Hodograph Cubic Splines

B. Jüttler

University of Technology, Darmstadt

Abstract

The article derives a method for matching G^1 Hermite data with Pythagorean hodograph cubics. We give a thorough discussion of the existence of solutions. This leads to a method for converting arbitrary space curves into cubic PH splines with the help of the Hermite interpolation procedure. Finally, the construction of rational frames for PH curves and rational approximations of rotation minimizing frames are outlined. The results have applications for sweep surface modeling in geometric design.

1 Introduction

Pythagorean hodograph (PH) curves are a special class of polynomial curves. They are characterized by the fact that their hodograph (that is, their tangent vector) corresponds to a rational curve on the unit sphere. This leads to a number of nice properties. For instance, the arc length of a PH curve is a polynomial function of the curve parameter.

Pythagorean hodograph curves have been studied in a number of publications by Farouki and co-authors, see e.g. [5]. A number of interpolation scheme for PH curves is available. Interpolation of planar G^1 Hermite data with planar PH quintics has been discussed in [4]. A construction for planar C^2 PH spline curves from point data has been developed by Farouki and Albrecht [1]. In addition, Wagner and Ravani [16] present a method for matching spatial G^1 Hermite data with PH space cubics. Their approach is based on certain geometric properties of the Bézier control polygon of PH space cubics which were revealed by Farouki and Sakkalis [5].

In the first part of paper we present another approach to G^1 Hermite interpolation with spatial PH curves. The hodographs of the PH curves are constructed at first; they describe rational curves on the unit sphere. Our

method is based on the generalized stereographic projection, see [3]. This mapping is very powerful tool for constructing rational parameterizations of quadric surfaces. As the main result, we obtain a simple characterization of feasible G^1 Hermite data for interpolation with PH cubics; the difference vector of the segment end points has to be contained within a certain quadratic cone which depends solely on the tangent vectors. As a consequence from this characterization of feasible data it is shown, that any space curve without flat points (i.e., $\kappa \neq 0$) can be approximated by a G^1 cubic PH spline curve as accurately as desired, provided that the number of segments is chosen big enough.

In the second part of the paper we give an outline of the construction of rational approximations to the rotation minimizing frame (cf. [11]) of a PH spline curve. This frame is used for generating so–called sweeping surfaces. Such surfaces are interesting for geometric modeling applications; they are generated by moving a profile curve along a given spine curve.

The rotation minimizing frame of a curve has been introduced into computer aided geometric design by Klok [11]. He constructs a piecewise linear surface which approximates the rotation minimizing sweeping surface. Recently, a more sophisticated method has been proposed by Wang and Joe [18]. Firstly, they convert the given curve into a biarc spline curve. Then, the sweeping surface is approximated by segments of surfaces of revolution which are pieced together to form a G^1 surface. Of course, the spine curve the resulting surface is piecewise planar curve.

With the help of PH spline curves it is possible to construct rational approximations to the rotation minimizing frame with non–planar spine curves. Firstly it is shown, that any PH curve has an associated rational frame. The existence of such a frame has already been observed by Farouki and Sakkalis [5]. Our proof is based on the very close connection between the generalized stereographic projection and the so–called Euler parameters of orthogonal matrices. It leads to an explicit formula for the possible rational frames of PH curves.

An approximation to the rotation minimizing frame of the curve can now be constructed by composing the rational frame of the PH curve with suitable rotations around the tangent. This leads to rational approximation of the rotation minimizing frame, hence to approximate rational representations (that is, NURBS representations) of the generated sweeping surfaces. The method is illustrated by an example.

2 Preliminaries

In order to make this article self–contained we briefly summarize some results from [3] concerning the construction of rational curves on the unit

sphere.

Points in Euclidean 3–space will be described by their Cartesian coordinates $\mathbf{y} = (y_1 \; y_2 \; y_3)^\top \in \mathbb{R}^3$. Sometimes, however, it will be advantageous to use the so–called homogeneous coordinates $\tilde{\mathbf{y}} = (\tilde{y}_0 \; \tilde{y}_1 \; \tilde{y}_2 \; \tilde{y}_3)^\top$ instead, where $\tilde{\mathbf{y}} \neq (0 \; 0 \; 0 \; 0)^\top$. The last three components of the homogeneous coordinates will be collected into the vector $\vec{\mathbf{y}} = (\tilde{y}_1 \; \tilde{y}_2 \; \tilde{y}_3)^\top$. For homogeneous coordinates with $\tilde{y}_0 \neq 0$, the corresponding Cartesian coordinates can be obtained from

$$\mathbf{y} = \frac{1}{\tilde{y}_0} \, \vec{\mathbf{y}} = (\frac{\tilde{y}_1}{\tilde{y}_0} \; \frac{\tilde{y}_2}{\tilde{y}_0} \; \frac{\tilde{y}_2}{\tilde{y}_0})^\top. \tag{2.1}$$

On the other hand, consider a given point with the Cartesian coordinates $\mathbf{y}$. For any real $\lambda \neq 0$, the set of linearly dependent homogeneous coordinate vectors $\lambda \tilde{\mathbf{y}}$ with $\tilde{y}_0 = 1$ and $\vec{\mathbf{y}} = \mathbf{y}$ describe this point.

Homogeneous coordinate vectors with $\tilde{y}_0 = 0$ correspond to points at infinity; they can be identified with the equivalence classes of parallel lines. By introducing the points at infinity, we use the projective extension of Euclidean 3–space. See [14] for more information on the use of homogeneous coordinates in geometry.

In order to construct rational parameterizations of the unit sphere

$$y_1^2 + y_2^2 + y_3^2 = 1, \tag{2.2}$$

or, if represented in homogeneous coordinates,

$$\tilde{y}_1^2 + \tilde{y}_2^2 + \tilde{y}_3^2 = \tilde{y}_0^2, \tag{2.3}$$

the so–called generalized stereographic projection δ has been introduced by Dietz et al. [3]. It maps the point $\tilde{\mathbf{p}} = (\tilde{p}_0 \; \tilde{p}_1 \; \tilde{p}_2 \; \tilde{p}_3)^\top$ to the point with the homogeneous coordinates

$$\delta(\tilde{\mathbf{p}}) = \begin{pmatrix} \tilde{p}_0^2 + \tilde{p}_1^2 + \tilde{p}_2^2 + \tilde{p}_3^2 \\ 2\tilde{p}_0\tilde{p}_1 - 2\tilde{p}_2\tilde{p}_3 \\ 2\tilde{p}_1\tilde{p}_3 + 2\tilde{p}_0\tilde{p}_2 \\ \tilde{p}_1^2 + \tilde{p}_2^2 - \tilde{p}_0^2 - \tilde{p}_3^2 \end{pmatrix}. \tag{2.4}$$

As the homogeneous coordinates $\tilde{\mathbf{y}} = \delta(\tilde{\mathbf{p}})$ fulfill the equation (2.3) of the unit sphere, the mapping δ maps any point $\tilde{\mathbf{p}}$ to a point on the sphere. The mapping δ can be thought of as a generalization of the stereographic projection; if it is restricted to the plane $p_3 = 0$ then we get the stereographic projection with the centre $\tilde{\mathbf{n}} = (1 \; 0 \; 0 \; 1)^\top$ at the 'north pole' of the sphere; each point $\tilde{\mathbf{p}}$ of the plane is mapped to the intersection of the line passing through $\tilde{\mathbf{n}}$ and $\tilde{\mathbf{p}}$ with the sphere.

Of course, the mapping δ cannot be a one–to–one mapping, as the sphere is a 2-dimensional manifold. Consider all points in 3–space which

are mapped to a certain point $\tilde{\mathbf{y}} = (\ \tilde{y}_0\ \tilde{y}_1\ \tilde{y}_2\ \tilde{y}_3\ )^\top$ on the sphere. It turns out that all these points form a line in 3–space. This line will be called a *projecting line* of the generalized stereographic projection. If $\tilde{\mathbf{y}}$ is not the north pole of the unit sphere, then the projecting line is

$$\lambda\ \sigma(\tilde{\mathbf{y}}) + \mu\ \rho(\tilde{\mathbf{y}}) \quad (\lambda, \mu \in \mathbb{R}) \tag{2.5}$$

where $\sigma(\tilde{\mathbf{y}})$ and $\rho(\tilde{\mathbf{y}})$ are the two points

$$\sigma(\tilde{\mathbf{y}}) = \begin{pmatrix} \tilde{y}_0 - \tilde{y}_3 \\ \tilde{y}_1 \\ \tilde{y}_2 \\ 0 \end{pmatrix} \text{ and } \rho(\tilde{\mathbf{y}}) = \begin{pmatrix} 0 \\ \tilde{y}_2 \\ -\tilde{y}_1 \\ \tilde{y}_0 - \tilde{y}_3 \end{pmatrix} \tag{2.6}$$

in 3–space. In fact, a short calculation confirms that

$$\delta(\ \lambda\ \sigma(\tilde{\mathbf{y}}) + \mu\ \rho(\tilde{\mathbf{y}})\ ) = 2\ (\lambda^2 + \mu^2)\ (\tilde{y}_0 - \tilde{y}_3)\ \tilde{\mathbf{y}}, \tag{2.7}$$

provided that the point $\tilde{\mathbf{y}}$ fulfills the equation of the unit sphere. The inverse image of the north pole is the line at infinity of the plane $\tilde{p}_3 = 0$, i.e., it is given by all points $(0\ \tilde{p}_1\ \tilde{p}_2\ 0)^\top$. The system projecting lines form a so–called elliptic linear congruence of lines, see [3] for more details.

Consider a segment of a spherical rational curve of even degree $2n$. With the help of homogeneous coordinates, it can be represented as

$$\tilde{\mathbf{y}}(t) = \sum_{i=0}^{2n} \tilde{\mathbf{c}}_i\ B_i^{2n}(t), \quad t \in [0,1], \tag{2.8}$$

with the Bernstein polynomials $B_l^k(t) = \binom{k}{l} t^l (1-t)^{k-l}$. Its four components $\tilde{y}_0(t), \ldots, \tilde{y}_3(t)$ are polynomials of degree $2n$ in Bernstein–Bézier representation, see [7]. The coefficient vectors $\tilde{\mathbf{c}}_i \in \mathbb{R}^4$ are the weighted control points of this representation, where the components $\tilde{c}_{i,0}$ are the weights. The curve (2.8) is a spherical curve if and only if its components fulfill the equation of the unit sphere (2.3) for all $t \in \mathbb{R}$.

According to an algebraic result on Pythagorean quadruples in polynomial rings, any spherical rational curve of degree $2n$ can be constructed by applying the generalized stereographic projection δ to a space curve

$$\tilde{\mathbf{p}}(t) = \sum_{i=0}^{n} \tilde{\mathbf{d}}_i\ B_i^n(t), \quad t \in [0,1], \tag{2.9}$$

of degree n, see [3]. For instance, any circle (which is a rational spherical curve of degree 2) can be obtained simply by mapping a line (represented as a rational Bézier curve of degree 1) to the sphere.

Let ϕ be an angle with $0 < \phi < \pi$ and let $c = \cos\phi$ and $s = \sin\phi$. Consider the two points

$$\tilde{\mathbf{t}}_0 = \begin{pmatrix} 1 \\ 0 \\ s \\ c \end{pmatrix} \quad \text{and} \quad \tilde{\mathbf{t}}_1 = \begin{pmatrix} 1 \\ 0 \\ -s \\ c \end{pmatrix} \tag{2.10}$$

on the unit sphere. There is a one–parametric system of circular arcs connecting both points. Each circular arc can be described by the homogeneous coordinates of a spherical rational curve of degree 2. For each circular arc, this representation provides another two degrees of freedom. The first one is due to the different parameterizations of the circular arc. The second one results from possible scalings of the homogeneous coordinates. Thus, we have a 3–parametric system of homogeneous coordinates for the quadratic rational representations of the circular arcs connecting $\tilde{\mathbf{t}}_0$ and $\tilde{\mathbf{t}}_1$. These possible representations can be constructed by applying the generalized stereographic projection δ to one of the line segments

$$\tilde{\mathbf{p}}_{\lambda,v,w}(t) = (1-t)\, v\, \sigma(\tilde{\mathbf{t}}_0) + t\, w\, (\, \sigma(\tilde{\mathbf{t}}_1) + \lambda\, \rho(\tilde{\mathbf{t}}_1)\,), \qquad t \in [0,1]. \tag{2.11}$$

The three parameters λ, v, w represent the three degrees of freedom. The weights $v \neq 0$ and $w \neq 0$ control the different parameterization and the possible scaling of the homogeneous coordinates of the circular arc. The parameter λ selects one of the possible circular arcs through the points $\tilde{\mathbf{t}}_0$ and $\tilde{\mathbf{t}}_1$. A short calculation leads to the rational Bernstein–Bézier representation of these circles,

$$\tilde{\mathbf{y}}(t) = \delta(\tilde{\mathbf{p}}_{\lambda,v,w}) = B_0^2(t)\, \tilde{\mathbf{c}}_0 + B_1^2(t)\, \tilde{\mathbf{c}}_1 + B_2^2(t)\, \tilde{\mathbf{c}}_2 \tag{2.12}$$

with the three control points

$$\tilde{\mathbf{c}}_0 = 2\, v^2\, (1-c)\, \tilde{\mathbf{t}}_0, \quad \tilde{\mathbf{c}}_2 = 2\, w^2\, (\lambda^2+1)\, (1-c)\, \tilde{\mathbf{t}}_1, \tag{2.13}$$

and

$$\tilde{\mathbf{c}}_1 = 2\, v\, w\, (c-1) \begin{pmatrix} c \\ \lambda\, s \\ 0 \\ 1 \end{pmatrix}. \tag{2.14}$$

An example is shown in Figure 1. It shows some of the circular arcs which connect two points on the unit sphere, and also the Bézier control polygons of the corresponding rational Bézier curves of degree 2. The possible middle control points $\tilde{\mathbf{c}}_1$ belong to the line where the tangent planes of the sphere at $\tilde{\mathbf{t}}_0$ and $\tilde{\mathbf{t}}_1$ intersect. The representation (2.12), (2.13) of the system of circles connecting the points $\tilde{\mathbf{t}}_0$ and $\tilde{\mathbf{t}}_1$ will be used for constructing cubic PH spline curves from G^1 Hermite data.

FIGURE 1. Bézier representation of the circular arcs connecting two points on the sphere.

3 PH curves

Consider a polynomial (also called an integral) Bézier curve of degree n,

$$\mathbf{x}(t) = \sum_{i=0}^{n} \mathbf{b}_i \, B_i^n(t), \quad t \in [0,1]. \tag{3.1}$$

with the control points $\mathbf{b}_i \in \mathbb{R}^3$, see [7]. A remarkable class of these curves is formed by the so–called Pythagorean hodograph (PH) curves, which have been studied by Farouki and co–authors in a number of publications [1, 4, 5]. They are characterized by the property that the length of the first derivative vector $\dot{\mathbf{x}}(t) = \mathrm{d}/\mathrm{d}t \, \mathbf{x}(t)$ is a *polynomial* function of the curve parameter t. Thus, the components $\dot{x}_1, \dot{x}_2, \dot{x}_3$ of the derivative belong to a Pythagorean quadruple; they satisfy the Diophantine equation

$$\dot{x}_1(t)^2 + \dot{x}_2(t)^2 + \dot{x}_3(t)^2 = p(t)^2, \tag{3.2}$$

where $p(t)$ is certain polynomial. As a consequence, the arc length of a PH curve is a polynomial function of the curve parameter; it is obtained as the integral of the polynomial $p(t)$.

Owing to (3.2), the curve with the homogeneous coordinates

$$\tilde{\mathbf{y}}(t) = (\, p(t) \; \dot{x}_1(t) \; \dot{x}_2(t) \; \dot{x}_3(t) \,)^\top \tag{3.3}$$

is a spherical rational curve. Thus, as any spherical rational curve can be constructed by applying the generalized stereographic projection δ to a space curve, we have the following result:

Lemma 1. *Consider a spatial rational curve $\tilde{\mathbf{p}}(t)$ of degree n, cf. (2.9). By applying the generalized stereographic projection δ to this curve we obtain a spherical rational curve $\tilde{\mathbf{y}}(t) = \delta(\tilde{\mathbf{p}}(t))$ of degree $2n$. Let $L(t)$ be a polynomial of degree k, and let $\mathbf{x}_0 \in \mathbb{R}^3$ be an arbitrary point. The spatial curve*

$$\mathbf{x}(t) = \mathbf{x}_0 + \int_0^t L(\tau)\, \vec{\mathbf{y}}(\tau)\, \mathrm{d}\tau \tag{3.4}$$

is a Pythagorean hodograph curve of degree $2n + k + 1$. Here, the integration is applied to the three components of the vector $L(\tau)\ \vec{\mathbf{y}}(\tau)$, and $\vec{\mathbf{y}}$ is the vector $(\ \tilde{y}_1\ \tilde{y}_2\ \tilde{y}_3\ )^\top$.

Due to the algebraic properties of the mapping δ, any PH curve can be obtained from this construction. More precisely, any PH curve of degree m can be obtained by choosing a degree n space curve and a polynomial of degree k such that $m = 2n + k + 1$. In particular, any cubic PH curve which is not a straight line segment can be obtained as the integral of a spherical curve of degree 2, i.e., by choosing the degrees $n = 1$ and $k = 0$. In this case, one may always simply set $L = 1$; the possible scalings of $\vec{\mathbf{y}}(t)$ by constant factors can be obtained by a suitable choice of the homogeneous coordinates of $\tilde{\mathbf{p}}(t)$. In fact, for positive constants L one has $\delta(\sqrt{L}\,\tilde{\mathbf{p}}) = L\ \delta(\tilde{\mathbf{p}})$. On the other hand, the sign of $\vec{\mathbf{y}}(t)$ can be changed by permuting the components of $\tilde{\mathbf{p}}$,

$$\tilde{\mathbf{y}} = \begin{pmatrix} y_0 \\ | \\ \vec{\mathbf{y}} \\ | \end{pmatrix} = \delta\Big(\begin{pmatrix} p_0 \\ p_1 \\ p_2 \\ p_3 \end{pmatrix}\Big) \quad \Leftrightarrow \quad \tilde{\mathbf{y}}^* = \begin{pmatrix} y_0 \\ | \\ -\vec{\mathbf{y}} \\ | \end{pmatrix} = \delta\Big(\begin{pmatrix} p_1 \\ -p_0 \\ -p_3 \\ p_2 \end{pmatrix}\Big). \tag{3.5}$$

The choice of polynomials $\tilde{\mathbf{p}}$ and L with the degrees $n = 0$ and $k = 2$ leads to line segments which are represented as cubic Bézier curves. This case will be excluded from the following considerations.

4 Interpolation of G^1 Hermite data

We construct a PH cubic curve from given G^1 boundary data. For a curve segment, the segment end points $\mathbf{x}_0,\ \mathbf{x}_1 \in \mathbb{R}^3$ and the unit tangent vectors $\vec{\mathbf{t}}_0, \vec{\mathbf{t}}_1 \in \mathbb{R}^3$ at these points are given. We assume that the tangent vectors are neither parallel nor anti-parallel, i.e., $\vec{\mathbf{t}}_0 \times \vec{\mathbf{t}}_1 \neq \vec{\mathbf{0}}$. By switching to suitable Cartesian coordinates we may achieve that the tangent vectors have the form

$$\vec{\mathbf{t}}_0 = (\ 0\ s\ c\ )^\top \text{ and } \vec{\mathbf{t}}_1 = (\ 0\ -s\ c\ )^\top, \tag{4.1}$$

where $c = \cos\phi$ and $s = \sin\phi$, with an angle ϕ, $0 < \phi < \frac{\pi}{2}$, cf. (2.10). The angle between the oriented tangent directions is 2ϕ.

We want to interpolate the above G^1 boundary data with a cubic PH curve. That is, the curve $\mathbf{x}(t)$ is to satisfy the interpolation conditions

$$\mathbf{x}(0) = \mathbf{x}_0,\ \mathbf{x}(1) = \mathbf{x}_1,\ \dot{\mathbf{x}}(0) = \tau_0 \vec{\mathbf{t}}_0,\ \dot{\mathbf{x}}(1) = \tau_1 \vec{\mathbf{t}}_1, \tag{4.2}$$

for arbitrary positive constants τ_0, τ_1.

By combining Lemma 1 ($n = 1,\ k = 0$) with the result (2.12) on the rational Bernstein–Bézier representations of the circles connecting the points $\tilde{\mathbf{t}}_0$ and $\tilde{\mathbf{t}}_1$, we get a representation of the cubic PH curves which interpolate to the boundary tangents $\vec{\mathbf{t}}_0$ and $\vec{\mathbf{t}}_1$. The control points of these PH cubics are

$$\begin{gathered}\mathbf{b}_0 = \mathbf{x}_0,\ \ \mathbf{b}_1 = \mathbf{x}_0 + \tfrac{2}{3} v^2 (1-c) \begin{pmatrix} 0 \\ s \\ c \end{pmatrix},\ \ \mathbf{b}_2 = \mathbf{x}_0 + \tfrac{2}{3} v (1-c) \begin{pmatrix} -s\, w\, \lambda \\ v\, s \\ v c - w \end{pmatrix}, \\ \text{and}\ \ \mathbf{b}_3 = \mathbf{x}_0 + \tfrac{2}{3} (1-c) \begin{pmatrix} -v\, s\, w\, \lambda \\ s\,(-w^2 + v^2 - w^2 \lambda^2) \\ w^2 \lambda^2 c + v^2 c + w^2 c - w\, v \end{pmatrix}.\end{gathered} \tag{4.3}$$

In fact, a short calculation confirms that $\mathbf{b}_1 - \mathbf{b}_0 = \frac{2}{3} v^2 (1-c)\, \vec{\mathbf{t}}_0$ and $\mathbf{b}_3 - \mathbf{b}_2 = \frac{2}{3} w^2 (1-c)(1+\lambda^2)\, \vec{\mathbf{t}}_1$. The system (4.3) of PH cubics depends on the two weights v, w and on the parameter λ. The weights control the parameterization of the spherical curve $\tilde{\mathbf{y}}(t)$ and the normalization of the homogeneous coordinates. The parameter λ selects one of the possible spherical arcs connecting $\vec{\mathbf{t}}_0$ with $\vec{\mathbf{t}}_1$.

In order to solve the solve the G^1 Hermite interpolation problem, one has to choose the three parameters v, w, λ such that the interpolation condition

$$\mathbf{x}(1) = \mathbf{b}_3 = \mathbf{x}_1 \tag{4.4}$$

is satisfied. Let $\vec{\mathbf{d}} = (\, d_1\, d_2\, d_3\,)^\top$ be the difference vector of the given points, i.e., $\vec{\mathbf{d}} = \mathbf{x}_1 - \mathbf{x}_0$. Combining (4.3) and (4.4) we obtain the three nonlinear equations

$$\begin{gathered}-\tfrac{2}{3}(1-c)\, s\, v\, w\, \lambda = d_1, \quad \tfrac{2}{3}(1-c)\, s\,(-w^2 + v^2 - w^2\lambda^2) = d_2, \\ \text{and} \quad \tfrac{2}{3}(1-c)\,(w^2\lambda^2 c + v^2 c + w^2 c - w\, v) = d_3\end{gathered} \tag{4.5}$$

for the three unknowns w, v and λ. Of course, we are only interested in real solutions.

4.1 Existence of solutions

The difference vector $\vec{\mathbf{d}} = (\, d_1\, d_2\, d_3\,)^\top$ will be called *feasible* for the G^1 Hermite interpolation, if the equations (4.5) are fulfilled for certain real

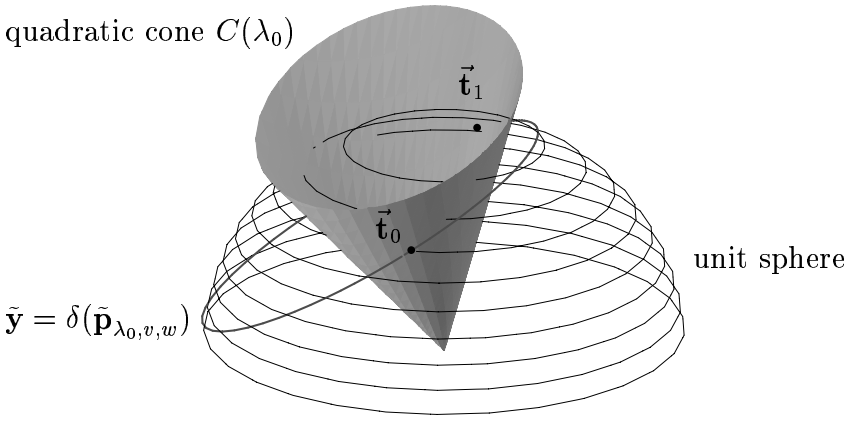

FIGURE 2. The quadratic cone of the feasible difference vectors for $\lambda = \lambda_0$.

values of w, v and λ.

Lemma 2. *The feasible difference vectors* $\vec{\mathbf{d}}$ *satisfy the quadratic equation*

$$(\, d_1\, d_2\, d_3\,) \underbrace{\begin{pmatrix} 4c^2+4c^2\lambda^2-1 & 0 & s\lambda \\ 0 & c^2\lambda^2 & 0 \\ s\lambda & 0 & (c-1)(c+1)\lambda^2 \end{pmatrix}}_{=C(\lambda)} \begin{pmatrix} d_1 \\ d_2 \\ d_3 \end{pmatrix} = 0 \quad (4.6)$$

for λ. *Thus, for any fixed parameter* $\lambda \in \mathbb{R}$, *the feasible difference vectors* $\vec{\mathbf{d}}$ *belong to a quadratic cone with its apex at the origin.*

The proof of this fact results simply by substituting (4.5) into (4.6). The matrix $C(\lambda)$ has been constructed by applying standard elimination techniques to the system (4.5), see e.g. [6].

As an example, the quadratic cone of the feasible difference vectors for a fixed parameter $\lambda = \lambda_0$ is depicted by Figure 2. Only the upper half of the cone (4.6) has been drawn; the other half is symmetric with respect to the plane $d_3 = 0$. The unit sphere is represented by some of its level curves $y_3 = \text{constant}$ (thin black lines). The black dots are the given unit tangents $\vec{\mathbf{t}}_0$ and $\vec{\mathbf{t}}_1$. The grey circle passing through the points $\vec{\mathbf{t}}_0$ and $\vec{\mathbf{t}}_1$ is the circle $\tilde{\mathbf{y}}(t) = \delta(\tilde{\mathbf{p}}_{\lambda_0,v,w}(t))$ which is formed by the unit tangent vectors of all PH cubics with $\lambda = \lambda_0$. All PH cubics with fixed $\lambda = \lambda_0$ are based on the same spherical circle, as the parameter λ selects one of the possible circular arcs connecting $\vec{\mathbf{t}}_0$ and $\vec{\mathbf{t}}_1$, see Section 2. The weights v and w, by contrast, control the various possible parameterizations and normalizations of the homogeneous coordinates $\tilde{\mathbf{y}}(t)$. The construction of Lemma 1 (with $L = 1$) leads to the feasible difference vectors, which form the quadratic cone $C(\lambda)$. The line $\mu\,\vec{\mathbf{t}}_0$, $\mu \in \mathbb{R}$ (and similarly $\mu\,\vec{\mathbf{t}}_1$)

is a generator of this cone, because choosing the weights $w = 0$, $v \neq 0$ would produce PH cubics which degenerate into line segments with the direction $\vec{\mathbf{t}}_0$. The spherical circle $\tilde{\mathbf{y}}(t)$ touches the quadratic cone from the outside.

For $\lambda = 0$, the spherical circle $\tilde{\mathbf{y}}(t)$ is the great circular arc which passes through $\vec{\mathbf{t}}_0$ and $\vec{\mathbf{t}}_1$. In this situation, the quadratic cone (4.6) degenerates into a double plane.

The components of $C(\lambda)$ are quadratic polynomials of the unknown parameter λ. Thus, the parameter λ can be computed as a one of the real roots (if they exist!) of (4.6).

Lemma 3. *Consider the given difference vector* $\vec{\mathbf{d}} = (\, d_1 \;\; d_2 \;\; d_3 \,)^\top$. *The quadratic equation (4.6) for the parameter* λ *has real roots if and only if one of the conditions*

$$4\,c^2\,(1-4\,c^2)\,{d_1}^2 + c^2\,(1-4\,c^2)\,{d_2}^2 + 4\,c^2\,s^2\,{d_3}^2 \geq 0 \tag{4.7}$$

or $d_1 = 0$ *is satisfied.*

The proof of this fact is simply based on the discriminant of the quadratic equation (4.6) for λ. This discriminant factorizes into $4\,{d_1}^2$ times the left–hand side of (4.7).

If the angle ϕ satisfies $1 - 4\,c^2 < 0$, i.e., $0 < \phi < \frac{\pi}{3}$, then the difference vectors which fulfill the inequality (4.7) form the interior of a quadratic cone with the apex at the origin. The cone is depicted in Figure 3. This cone is symmetric with respect to the y_1y_2–, y_1y_3–, and y_2y_3–plane. Its interior contains the y_3–axis, but neither the y_1 nor the y_2–axis. In addition, the given tangent directions $\vec{\mathbf{t}}_0$, $\vec{\mathbf{t}}_1$ belong to its interior, as

$$4\,c^2\,(1-4\,c^2)\,0^2 + c^2\,(1-4\,c^2)\,s^2 + 4\,c^2\,s^2\,c^2 = c^2 s^2 \geq 0. \tag{4.8}$$

The boundary of the quadratic cone (4.7) is the envelope of the system of quadratic cones (4.6), $\lambda \in \mathbb{R}$. The Figure 3 shows one of these cones; it touches the boundary of (4.7).

If the angle ϕ satisfies $1 - 4\,c^2 \geq 0$, i.e., $\frac{\pi}{3} \leq \phi \leq \frac{\pi}{2}$, then the condition (4.7) is fulfilled by all difference vectors $\vec{\mathbf{d}} \in \mathbb{R}^3$.

With the help of the quadratic equation (4.6), one can compute the unknown parameter λ from the given Hermite data. If the condition of Lemma 3 is fulfilled, then we get at least one real solution to (4.6). Now, in a second step, one has to assign suitable values to the weights v and w. In the remainder of this chapter we will derive suitable assumptions which guarantee the existence of real solutions for v and w.

For the sake of brevity we will consider only Hermite data with $\phi < \frac{\pi}{3}$. That is, the angle 2ϕ between the given tangent directions is assumed to

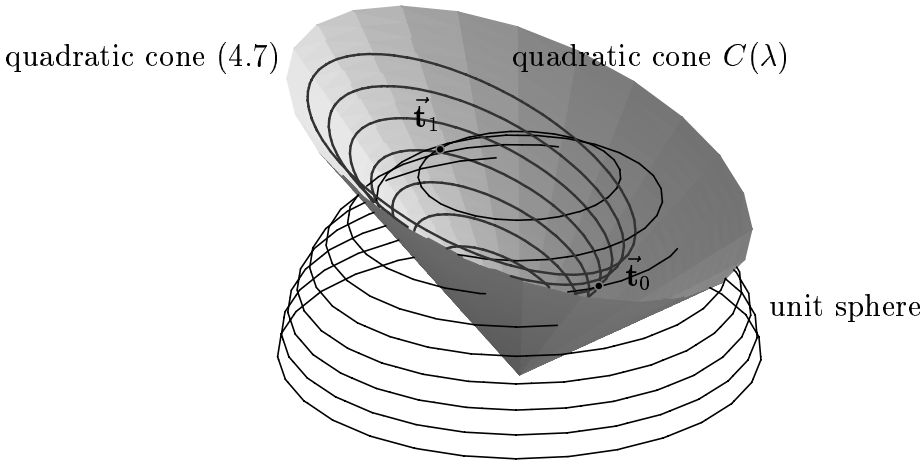

FIGURE 3. The cone (4.7) of difference vectors leading to real solutions of (4.6).

be smaller than 120°. This is the more interesting case for applications, as a large angle between adjacent tangents is not realistic. For instance, if one wishes to convert a given space curve into a PH cubic spline curve with the help of G^1 Hermite interpolation, then it is always possible to subdivide the original curve such that the above assumption gets true.

Owing to (4.5) the system $\vec{\mathbf{d}} = \vec{\mathbf{d}}(\lambda, v, w)$ of feasible difference vectors can be rewritten as

$$\begin{aligned} \vec{\mathbf{d}}(\lambda, v, w) = \begin{pmatrix} d_1 \\ d_2 \\ d_3 \end{pmatrix} &= v^2 \left[\tfrac{2}{3}(1-c)\, \vec{\mathbf{t}}_0 \right] - 2vw \left[\tfrac{1}{3}(1-c) \begin{pmatrix} s\lambda \\ 0 \\ 1 \end{pmatrix} \right] \\ &+ w^2 \left[\tfrac{2}{3}(1-c)(1+\lambda^2)\, \vec{\mathbf{t}}_1 \right] \end{aligned} \tag{4.9}$$

Resulting from this representation, one gets

$$\vec{\mathbf{d}}(\lambda, \xi\, v, \xi\, w) = \xi^2\, \vec{\mathbf{d}}(\lambda, v, w). \tag{4.10}$$

Thus, the set of feasible difference vectors is a collection of rays emanating from the origin $\vec{\mathbf{O}}$.

Lemma 4. *Any pair of weights $(v, w) \in \mathbb{R}^2$ can be represented as*

$$(v, w) = (t\,\xi, (1-t)\xi) \quad \textit{or as} \quad (v, w) = (t\,\xi, -(1-t)\xi) \tag{4.11}$$

with $t \in [0, 1]$ and $\xi \in \mathbb{R}$.

The proof results immediately by choosing $\xi = \pm(|v| + |w|)$.

Thus, the set of feasible difference vectors is the collection of rays emanating from the origin $\vec{\mathbf{O}}$ which are spanned by the two Bézier curves

$$\begin{aligned}\vec{\mathbf{d}}^{\,*}_{\pm}(\lambda,t) \;=\; & B_0^2(t)\;\tfrac{2}{3}(1-c)\,\vec{\mathbf{t}}_0 \pm B_1^2(t)\;\tfrac{1}{3}(1-c)\begin{pmatrix} s\lambda \\ 0 \\ 1 \end{pmatrix} \\ & +\; B_2^2(t)\;\tfrac{2}{3}(1-c)(1+\lambda^2)\,\vec{\mathbf{t}}_1, \qquad t\in[0,1].\end{aligned} \tag{4.12}$$

These curves result by substituting (4.11) with $\xi = 1$ into (4.9). The third components of these curves are strictly positive for $t \in [0,1]$,

$$\begin{aligned} & B_0^2(t)\,\tfrac{2}{3}\,(1-c)\,c \pm B_1^2(t)\,\tfrac{1}{3}\,(1-c) + B_2^2(t)\,(1-c)\,(1+\lambda^2)\,c \\ & \quad \geq \tfrac{2}{3}\,(1-c)\,[\,(1-t)^2\,c - t\,(1-t) + t^2\,c\,] \\ & \quad \geq \tfrac{2}{3}\,(1-c)\,[\,(1-t)^2\,c - 2\,t\,(1-t)\,c + t^2\,c\,] \\ & \quad = \tfrac{2}{3}\,(1-c)\,c\,[\,(1-t) - t\,]^2, \end{aligned} \tag{4.13}$$

as $\phi < \frac{\pi}{3}$ (hence $c > \frac{1}{2}$) is assumed.

Case 1: $\lambda \neq 0$. As shown in Lemma 2, the given difference vector $(\,d_1\;d_2\;d_3\,)^\top$ belongs to the quadratic cone (4.6). The y_1y_2–plane separates the upper and the lower half of this cone, as $\phi < \frac{\pi}{3}$ was assumed. This can be seen from the fact, that the plane $d_3 = y_3 = 0$ intersects the the cone (4.6) only at the origin, because both coefficients $C_{1,1}(\lambda)$ and $C_{2,2}(\lambda)$ are guaranteed to be positive.

On the other hand it can be seen from the (4.12), that the feasible difference vectors span the whole upper half of the quadratic cone (4.6). The middle control points of the two Bézier curves lie on either side of the plane $y_1 = 0$ which contains the remaining two control points.

Thus, if $\lambda \neq 0$, then real solutions for the weights v, w exist, provided that the given difference vector $\vec{\mathbf{d}} = (\,d_1\;d_2\;d_3\,)^\top$ satisfies $d_3 > 0$. In addition, it fulfills the condition of Lemma 3, as a real solution λ exists. We can even conclude that the first condition (4.7) of Lemma 3 has to be satisfied, because the only intersections of the cone (4.6) with the plane $d_1 = 0$ are the lines spanned by $\vec{\mathbf{t}}_0$ and $\vec{\mathbf{t}}_1$. As observed earlier, the points of both lines satisfy (4.7).

Case 2: $\lambda = 0$. The given difference vector $(\,d_1\;d_2\;d_3\,)^\top$ is contained in the plane $d_1 = 0$, because the cone (4.6) degenerates into this plane. Thus, the given Hermite data are planar; the tangent directions $\vec{\mathbf{t}}_0$, $\vec{\mathbf{t}}_1$ and the difference vector $\vec{\mathbf{d}}$ are coplanar.

We consider the two Bézier curves $\vec{\mathbf{d}}^{\,*}_{\pm}(0,t)$ in the plane $d_1 = 0$, which span the set of feasible difference vectors. See Figure 4 for an illustration. The extreme rays (dashed lines) of the feasible region are tangents of

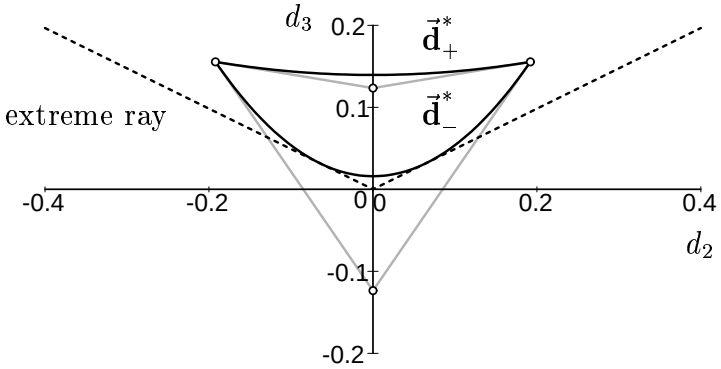

FIGURE 4. Feasible difference vectors for $\lambda = 0$.

the curve $\vec{\mathbf{d}}^*_-(0,t)$; their directions can be found by solving the quadratic equation $\det(\vec{\mathbf{d}}^*_-(0,t), \mathrm{d}/\mathrm{d}t\ \vec{\mathbf{d}}^*_-(0,t)) = 0$. This leads to the directions

$$(0 \quad \pm 2\,(c-1)s\sqrt{(2\,c-1)(2\,c+1)} \quad -(c-1)(2\,c-1)(2\,c+1)\ )^\top \qquad (4.14)$$

of the extreme rays. On the other hand, the lines which are spanned by these directions turn out to be the boundaries of the intersection of the quadratic cone (4.7) with the plane $d_1 = 0$, as the left–hand side of (4.7) vanishes for (4.14). Thus, for $\lambda \neq 0$ we get solutions to the Hermite interpolation problem provided that the given difference vector satisfies the inequalities (4.7) and $d_3 > 0$. In addition, it satisfies $d_1 = 0$, as $\lambda = 0$ holds. Hence, we have exactly the same conditions as in the previous case. This could have been concluded immediately from the fact, that the feasible difference vectors $\vec{\mathbf{d}}(\lambda, v, w)$ (see (4.9)) depend continuously on the parameters λ, v and w. However, the separate discussion of the planar case may be of some interest for dealing with planar PH curves.

Summarizing these observations we have the following result:

Theorem 5. *The G^1 Hermite interpolation problem with $0 < \phi < \frac{\pi}{3}$ has regular real solutions if and only of the difference vector $\vec{\mathbf{d}}$ satisfies the inequalities (4.7) and $d_3 > 0$. Thus, the difference vector has to be contained in the upper half of the quadratic cone (4.7), see also Figure 3.*

Proof. The regularity of the solutions remains to be shown. The given curve is regular if and only if the weights satisfy $v, w \neq 0$; under these assumptions we have $\vec{\mathbf{y}}(t) \neq \vec{\mathbf{0}}$, hence $\dot{\mathbf{x}} \neq \vec{\mathbf{0}}$, cf. (2.12) and Lemma 1.

Consider the case $v = 0$. Resulting from (4.5), the given difference vector $\vec{\mathbf{d}}$ is linearly dependent on $\vec{\mathbf{t}}_1$. Hence, by choosing $\lambda = 0$ one can find another solution (v, w) with $v, w \neq 0$. This solution is found by intersecting the curve $\vec{\mathbf{d}}^*_-(0,t)$ (see (4.12) and Figure 4) with the line

spanned by $\vec{\mathbf{t}}_1$; this leads to a point $\vec{\mathbf{d}}^*_-(0,t_0)$. According to (4.10), a regular solution of the Hermite interpolation can the be found by choosing $(v,w) = (\,\xi\, t_0, -\xi(1-t_0)\,)$, where ξ is found from $\vec{\mathbf{d}} = \xi^2\, \vec{\mathbf{d}}^*_-(0,t_0)$ This is possible as $d_3 > 0$ holds. Thus, if the system (4.5) has a solution with $v = 0$ (or, similarly, with $w = 0$), then there exists another regular solution with $\lambda = 0$. □

4.2 Computing the solutions

If the tangent vectors are not given in the standard form (4.1), then one has to convert the given Hermite data into a new coordinate system, whose p_1– (resp. p_3–) axis is perpendicular to (resp. the bisector of) both tangent directions.

Let $\vec{\mathbf{d}}_{\text{given}} = (\ X\ Y\ Z\ )^\top$ be the difference vector of the given segment end points $\mathbf{x}_0$ and $\mathbf{x}_1$. If the assumptions of Theorem 5 are satisfied, then we are able to compute a PH cubic which matches the given end points and tangent directions. In order to find the parameter λ and the weights v, w, one needs to discuss two cases.

Case 1. The data are not coplanar, i.e. $X \neq 0$. The parameter λ can be found from the quadratic equation (4.6). This yields the two solutions

$$\lambda_{1/2} = \frac{Z\, s \pm c\,\sqrt{16\, s^2X^2{+}4\, s^2Y^2{+}4\, s^2Z^2{-}12\, X^2{-}3\, Y^2}}{4\, s^2X^2{+}s^2Y^2{+}s^2Z^2{-}4\, X^2{-}Y^2}\, X. \tag{4.15}$$

Now consider the three quadratic equations

$$\vec{\mathbf{d}}(\lambda_k, v, w) \times \begin{pmatrix} X \\ Y \\ Z \end{pmatrix} = w^2\, \vec{\mathbf{d}}(\lambda_k,\ \frac{v}{w},\ 1) \times \begin{pmatrix} X \\ Y \\ Z \end{pmatrix} = \begin{pmatrix} 0 \\ 0 \\ 0 \end{pmatrix} \tag{4.16}$$

for the weight ratio v/w. Forming linear combinations of them one may find a linear equation for this ratio. This leads to $v/w = A_k/B_k$ with

$$A_k = 2\, c\, (1+\lambda^2)\, X \quad \text{and} \quad B_k = Y\, c\, \lambda + X - Z\, s\, \lambda, \quad k = 1, 2. \tag{4.17}$$

Now we compute the weights $v = v_k = \xi_k\, A_k$ and $w = w_k = \xi_k\, B_k$ from

$$\vec{\mathbf{d}}(\lambda_k, \xi_k\, A_k, \xi_k\, B_k) = (\xi_k)^2\ \vec{\mathbf{d}}(\lambda_k, A_k, B_k) = (\ X\ Y\ Z\ )^\top. \tag{4.18}$$

This gives

$$(\xi_k)^2 = \frac{3}{4\, s\, \lambda_k\, c(1+{\lambda_k}^2)\, (c-1)(Y\, c\, \lambda_k + X - Z\, s\, \lambda_k)}. \tag{4.19}$$

The sign of ξ_k can be chosen arbitrarily. The control points of the resulting PH cubic do not depend on the choice of the sign, see (4.3).

Case 2. The data are coplanar, $X = 0$. In this case we choose $\lambda = 0$. Consider the third component of the cross product

$$\begin{pmatrix} 0 \\ 0 \\ 0 \end{pmatrix} = \vec{\mathbf{d}}(\lambda_k, v, w) \times \begin{pmatrix} 0 \\ Y \\ Z \end{pmatrix} = w^2 \, \vec{\mathbf{d}}(\lambda_k, \, \frac{v}{w}, \, 1) \times \begin{pmatrix} 0 \\ Y \\ Z \end{pmatrix}. \qquad (4.20)$$

It leads to a quadratic equation with solutions $v/w = A_k/B_k$,

$$A_{1/2} = Y \pm \sqrt{4\,s^2\,Z^2 - 3\,Y^2 + 4\,s^2\,Y^2}, \quad B_{1/2} = 2\,(Y\,c - Z\,s). \qquad (4.21)$$

This computation fails iff $\vec{\mathbf{d}}_{\text{given}}$ depends linearly on $\vec{\mathbf{t}}_0$; then one has to use the ratio w/v instead.

Similar to the previous case we compute the weights $v = v_k = \xi_k\,A_k$ and $w = w_k = \xi_k\,B_k$ from

$$\vec{\mathbf{d}}(0, \xi_k\,A_k, \xi_k\,B_k) = (\xi_k)^2\;\vec{\mathbf{d}}(0, A_k, B_k) = (\;0\;Y\;Z\;)^\top. \qquad (4.22)$$

This gives

$$(\xi_k)^2 = \frac{3}{4\,s(1-c)(4\,Z\,c\,s - 3\,Y + 4\,s^2\,Y \pm \sqrt{4\,s^2\,Z^2 - 3\,Y^2 + 4\,s^2\,Y^2})}, \qquad (4.23)$$

$k = 1, 2$. Again, the sign of ξ_k is arbitrary.

In both cases we get two solutions (λ_k, v_k, w_k), $k = 1, 2$. We choose the one where the length of the circular arc (2.12) (which is formed by the unit tangent vectors of the PH cubics) is smaller. This is the solution where $v\,w < 1$. The weight weight $2(c-1)v\,w$ of the middle control points $\tilde{\mathbf{c}}_1$ is then positive.

Note that the solutions depend continuously on the data, because the function $\vec{\mathbf{d}}(\lambda, v, w)$ is a continuous function of the parameters and weights λ, v and w. Thus, if the data converge from the spatial to the planar situation, then the solutions to spatial data will converge to solutions to the planar data. However, if the data are close to the planar situation, then one has to take extra care in order to avoid numerical problems.

As an alternative approach to the computation, one may use the control–point based technique which has been developed by Wagner and Ravani [16]. This approach, however, does not yield any information about the pre–image of the interpolating PH cubic for the generalized stereographic projection. For the approximate computation of rotation minimizing frames as outlined below, it is essential to use this additional information which is only provided by the first scheme. In addition, the existence of real solutions can better be discussed with our approach.

5 Converting space curves into PH splines

Consider a given space curve segment $\mathbf{p} = \mathbf{p}(t)$ with the parameter t varying in the interval $[0, S]$. One may assume that the parameter t is the arc length of the curve, i.e. $\|\vec{\mathbf{t}}(t)\| = \|\dot{\mathbf{p}}(t)\| \equiv 1$ holds, see [12]. With the help of the G^1 Hermite interpolation procedure, we want to convert the given curve into a sequence of PH cubics. Firstly, for a given step-size $\Delta = S/N$, we generate a sequence of points $\mathbf{p}(i\,\Delta)$ with associated unit tangent vector $\vec{\mathbf{t}}(i\,\Delta)$, $i = 0, \ldots, N$. Secondly, we apply the above described Hermite interpolation procedure to each pair of adjacent G^1 Hermite data $\mathbf{p}(i\,\Delta), \vec{\mathbf{t}}(i\,\Delta)$ and $\mathbf{p}(\,(i{+}1)\,\Delta), \vec{\mathbf{t}}(\,(i{+}1)\,\Delta)$. If the assumptions of Theorem 5 are satisfied for each segment, then this leads to a PH cubic spline curve. In the sequel we discuss the following question.

Is it always possible to convert the given curve $\mathbf{p}(t)$ *into a cubic PH spline with any desired accuracy via* G^1 *Hermite interpolation?*

In order to answer this question, one has to discuss the asymptotic behaviour of the solutions to the Hermite interpolation problem for $\Delta \to 0$. We consider the given curve in a neighbourhood of a point $\mathbf{p}(t_0)$. Under suitable assumptions about its differentiability, the curve can be represented by its canonical Taylor expansion

$$\mathbf{p}(t) = \begin{pmatrix} (t{-}t_0) - \frac{1}{6}\,\kappa_0^2\,(t{-}t_0)^3 + O((t{-}t_0)^4) \\ \frac{1}{2}\,\kappa_0\,(t{-}t_0)^2 + \frac{1}{6}\,\kappa_1\,(t{-}t_0)^3 + O((t{-}t_0)^4) \\ \frac{1}{6}\,\kappa_0\,\tau_0\,(t{-}t_0)^3 + O((t{-}t_0)^4) \end{pmatrix} \tag{5.1}$$

which results from the well–known Frenet formulas, see [12]. Here, the origin of the coordinate system is at $\mathbf{p}(t_0)$, the p_1–axis is spanned by $\vec{\mathbf{t}}(t_0)$, and the p_1p_2–plane is the osculating plane of the curve at $\mathbf{p}(t_0)$. The coefficients κ_i, τ_j are the derivatives of curvature and torsion at $t = t_0$,

$$\kappa_i = \frac{\mathrm{d}^i}{\mathrm{d}t^i}\kappa(t)\bigg|_{t=t_0} \quad \text{and} \quad \tau_j = \frac{\mathrm{d}^j}{\mathrm{d}t^j}\tau(t)\bigg|_{t=t_0}. \tag{5.2}$$

The curve points $\mathbf{p}(t_0)$, $\mathbf{p}(t_0+\Delta)$ with the associated unit tangent vectors $\vec{\mathbf{t}}(t_0)$, $\vec{\mathbf{t}}(t_0+\Delta)$ are to be interpolated with a PH cubic.

Firstly, in order to apply the formulas from the previous section, we have to transform the data into the local coordinate system. Its x_1–axis (resp. x_3–axis) has the direction $\vec{\mathbf{t}}(t_0) \times \vec{\mathbf{t}}(t_0+\Delta)$ (resp. $\vec{\mathbf{t}}(t_0) + \vec{\mathbf{t}}(t_0+\Delta)$). With the help of computer algebra tools one gets Taylor expansions for $c = \cos\phi$, $s = \sin\phi$, and for the components X, Y, Z of the difference

vector $\vec{\mathbf{d}}_{\text{given}} = \mathbf{p}(t_0 + \Delta) - \mathbf{p}(t_0)$ of the segment end points:

$$\begin{aligned} c &= 1 - \tfrac{1}{8}\,\kappa_0^2\,\Delta^2 - \tfrac{1}{8}\,\kappa_0\,\kappa_1\,\Delta^3 + O(\Delta^4), \\ s &= \tfrac{1}{2}\,\kappa_0\,\Delta + \tfrac{1}{4}\,\kappa_1\,\Delta^2 + \tfrac{1}{12}\,(\kappa_2 - \tfrac{1}{4}\,\kappa_0\,\tau_0^2 - \tfrac{1}{4}\,\kappa_0^3)\,\Delta^3 + O(\Delta^4), \\ X &= \tfrac{1}{12}\,\kappa_0\,\tau_0\,\Delta^3 + O(\Delta^4), \\ Y &= \tfrac{11}{12}\,\kappa_1\,\Delta^3 + O(\Delta^4) \quad \text{and} \\ Z &= \Delta - \tfrac{1}{24}\,\kappa_0^2\Delta^3 + O(\Delta^4). \end{aligned} \tag{5.3}$$

Now we can check whether the conditions of Theorem 5 become true if the stepsize Δ converges to zero.

Obviously, the second condition $Z = d_3 > 0$ gets true for sufficiently small Δ. On the other hand, the left–hand side of the inequality (4.7) has the Taylor expansion

$$\kappa_0^2\,\Delta^4 + \kappa_0\,\kappa_1\,\Delta^5 + O(\Delta^6). \tag{5.4}$$

Thus, solutions for sufficiently small stepsize Δ are guaranteed to exist, provided that the curve has non–zero curvature at $\mathbf{p}(t_0)$, i.e. $\kappa_0 \neq 0$.

We give a brief geometric interpretation of this fact. Consider the angle between the difference vector $\vec{\mathbf{d}}_{\text{given}}$ and the p_3–axis of the local coordinate system. It has the Taylor expansion

$$\tfrac{1}{12}\,\sqrt{\kappa_0\,\tau_0^2 + 121\,\kappa_1^2}\,\Delta^2 + O(\Delta^4), \tag{5.5}$$

hence it converges *quadratically* to zero. On the other hand, consider the quadratic cone (4.7) of the feasible difference vectors. This cone is centrally symmetric with respect to the p_3–axis of the local coordinate system. It intersects the p_1p_3– and p_2p_3–plane in a pair of lines. The angles between these lines and the z–axis have the expansions

$$\tfrac{1}{3}\,\sqrt{6}\,\kappa_0\,\Delta\, + O(\Delta^2) \quad \text{and} \quad \tfrac{1}{6}\,\sqrt{6}\,\kappa_0\,\Delta\, + O(\Delta^2), \tag{5.6}$$

they converge *linearly* to zero for $\Delta \to 0$. Thus, if $\kappa_0 \neq 0$, then solutions to the Hermite interpolation problem exist, provided that the stepsizes Δ are sufficiently small.

Next we consider briefly the asymptotic behaviour of the solutions for decreasing stepsize $\Delta \to 0$. The two possible values of the parameter λ have the Taylor expansions

$$\lambda_1 = \tfrac{1}{2}\,\tau_0\,\Delta - \tfrac{1}{4}\,\tau_1\Delta^2 + O(\Delta^3) \;\text{ and }\; \lambda_2 = -\tfrac{1}{6}\,\tau_0\,\Delta - \tfrac{1}{12}\,\tau_1\Delta^2 + O(\Delta^3) \tag{5.7}$$

Owing to (4.3), the interpolating PH cubic has the control points

$$\begin{gathered} \mathbf{b}_0 = \mathbf{p}(t_0), \quad \mathbf{b}_1 = \mathbf{p}(t_0) + l_1\,\vec{\mathbf{t}}(t_0), \\ \mathbf{b}_2 = \mathbf{p}(t_0 + \Delta) - l_2\,\vec{\mathbf{t}}(t_0 + \Delta), \quad \text{and} \quad \mathbf{b}_3 = \mathbf{p}(t_0 + \Delta), \end{gathered} \tag{5.8}$$

with the lengths $l_1 = \frac{2}{3}v^2(1-c)$ and $l_2 = \frac{2}{3}w^2(1-c)(1+\lambda^2)$. If we use the first solution $\lambda = \lambda_1$, then both lengths are asymptotically equal to

$$l_{1,1} = l_{2,1} = \frac{1}{3}\Delta + O(\Delta^2). \tag{5.9}$$

For this solution, the length of the spherical curve (2.12) which is formed by the unit tangent vectors of the interpolating PH cubic tends to zero. For decreasing stepsize $\Delta \to 0$, the first solution converges to the solution of C^1 Hermite interpolation with standard cubic Bézier curves, where the given curve $\mathbf{p}(t)$ is parameterized with respect to its arc length.

For the second solution $\lambda = \lambda_2$, by contrast, we get $l_{1,2} = l_{2,2} = \Delta + O(\Delta^2)$. In this case, the length of the spherical curve (2.12) which is formed by the unit tangent vectors converges to $2\,\pi$. The first solution is to be preferred, as the shape of the resulting spline curves is much better.

The asymptotic behaviour of both solutions is depicted in Figure 5. The original curve segment has been drawn in grey. The solid (resp. dashed) curve show the cubic Bézier curve which is obtained from the first (resp. second) solution of the G^1 Hermite interpolation problem.

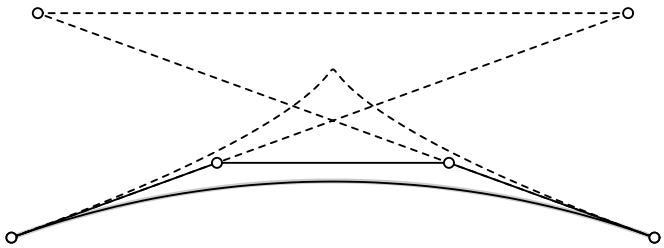

FIGURE 5. Asymptotic behaviour of the two solutions (scheme)

For each point $\mathbf{p}(t_0)$ of the given curve we can find a maximum stepsize $\Delta_{\max}(t_0)$, such that the solution to the Hermite interpolation problem with the point and tangent data $\mathbf{p}(t_0)$, $\mathbf{p}(t_0+\Delta)$ and $\vec{\mathbf{t}}(t_0)$, $\vec{\mathbf{t}}(t_0+\Delta)$ exists for any stepsize $\Delta \in [0, \Delta_{\max}(t_0)]$. We assume that the curvature $\kappa(t_0)$ is strictly positive for all $t_0 \in [0, s]$. (For space curves, the sign of the curvature has no meaning, see [12]). Under this assumption, the maximum stepsize will be positive, $\Delta_{\max}(t_0) > 0$. Moreover, there exists a global lower bound Δ_0 for the maximum stepsize,

$$\Delta_{\max}(t_0) \geq \Delta_0 > 0, \tag{5.10}$$

as we are dealing with a curve segment of finite length S. Summing up, we have the following result:

Consider a given curve segment $\mathbf{p}(t)$, $t \in [0, S]$ *of finite length which is*

sufficiently often differentiable or which is a collection of segments which are sufficiently often differentiable. (The latter assumption is satisfied by the curve representations of CAD systems.) *The curvature of the curve is assumed to be strictly positive. With the help of G^1 Hermite interpolation with PH cubics as described in the previous section, this curve can be approximately converted into a PH cubic spline curve. By increasing the number of segments, the approximation can be made as highly accurate as desired.*

For practical implementations, one should use an adaptive choice of the stepsize, in order to keep the number of segments as small as possible. In the neighbourhood of points with $\kappa = 0$, one will have to use smaller stepsizes in order to get close to such points. For true space curves, such points are very unlikely to occur. This, however, is different in the planar case, where inflections may happen quite frequently.

6 Rational frames of PH curves

Consider a segment of a space curve $\mathbf{x}(t)$ and a matrix–valued function $U = U(t)$, both with the parameter $t \in [0,1]$. The matrix $U(t)$ is assumed to be a special orthogonal matrix for all t, i.e., it satisfies $U\,U^\top = I$ and $\det U = +1$. The mapping

$$\mathbb{R}^3 \times [0,1] \to \mathbb{R}^3 \quad (\mathbf{q}, t) \mapsto \mathbf{q}'(t) = \mathbf{x}(t) + U(t)\,\mathbf{q} \tag{6.1}$$

describes a spatial Euclidean *motion*. The parameter t can be identified with the time. The coordinate vectors $\mathbf{q}$ and $\mathbf{q}'$ describe the points of the *moving* and of the *fixed* system, respectively. Owing to the properties of the matrix U, the motion preserves (for each t) the distances between points. The origin $\mathbf{O}$ of the moving system travels along the curve $\mathbf{x}(t)$.

The motion (6.1) will be called a *frame* of the given curve $\mathbf{x}(t)$, if the vectors

$$U(t) \begin{pmatrix} 0 \\ 0 \\ 1 \end{pmatrix} \quad \text{and} \quad \dot{\mathbf{x}}(t) \tag{6.2}$$

are linearly dependent for all $t \in [0,1]$. Under this assumption, the p_1p_2–plane of the moving system is always mapped onto the normal plane of the given curve $\mathbf{x}(t)$. For instance, the well–known Frenet frame of a space curve is obtained by choosing the orthogonal matrix $U = [\vec{\mathbf{n}}(t)\,\vec{\mathbf{b}}(t)\,\vec{\mathbf{t}}(t)]$. Here, the vectors $\vec{\mathbf{n}}$, $\vec{\mathbf{b}}$ and $\vec{\mathbf{t}}$ are the normal, the binormal, and the tangent vector of the curve, see [12].

Frames of space curves are used for sweep surface modeling in geometric design. Consider a planar curve segment $\mathbf{c} = \mathbf{c}(u)$, $u \in [0,1]$, in the

p_1p_2–plane of the moving system, i.e. $c_3(u) \equiv 0$. Then, the surface

$$\mathbf{x}(t) + U(t)\,\mathbf{c}(u), \qquad (u,t) \in [0,1]^2, \tag{6.3}$$

is a so–called sweeping surface; all parameter lines $t = \text{const.}$ are congruent. The generating curve $\mathbf{c}(u)$ is the *profile curve* of the surface. The trajectory $\mathbf{x}(t)$ is sometimes referred to as the *spine curve*. If the surface is generated by a *frame* rather than a general motion, then the parameter lines $t = \text{const.}$ lie in the normal planes of the curve $\mathbf{x}(t)$. See [11, 15, 18] for more information on frames and sweep surface modeling.

The motion (6.1) is said to be a *rational* motion, if both the components of $\mathbf{x}$(t) and the components of the matrix $U(t)$ are rational functions of the parameter t. Under this assumption, the trajectories of the points of the moving system are rational curves. Also, if $\mathbf{c}(t)$ is a rational curve, then so is the sweeping surface (6.3). Rational motions which satisfy (6.2) are called rational frames. For more information about rational motions the reader is referred to [10].

The following fact has firstly been observed by Farouki and Sakkalis [5].

Lemma 6. *Any PH curve has a rational frame.*

With the help of the generalized stereographic projection, we give another proof of this observation. In addition, the proof leads to an explicit formula for the rational frames of PH curves, see (6.5).

Proof. As observed earlier in Section 3, any PH curve can be obtained from the construction which is described by Lemma 1. Let $\tilde{\mathbf{p}}(t)$ be the homogeneous coordinates of the preimage curve. The matrix

$$U_0 = \frac{1}{D}\begin{pmatrix} -\tilde{p}_0^2+\tilde{p}_1^2-\tilde{p}_2^2+\tilde{p}_3^2 & -2\,\tilde{p}_0\,\tilde{p}_3-2\,\tilde{p}_1\,\tilde{p}_2 & -2\,\tilde{p}_2\,\tilde{p}_3+2\,\tilde{p}_0\,\tilde{p}_1 \\ -2\,\tilde{p}_0\,\tilde{p}_3+2\,\tilde{p}_1\,\tilde{p}_2 & \tilde{p}_0^2+\tilde{p}_1^2-\tilde{p}_2^2-\tilde{p}_3^2 & 2\,\tilde{p}_0\,\tilde{p}_2+2\,\tilde{p}_1\,\tilde{p}_3 \\ -2\,\tilde{p}_2\,\tilde{p}_3-2\,\tilde{p}_0\,\tilde{p}_1 & 2\,\tilde{p}_0\,\tilde{p}_2-2\,\tilde{p}_1\,\tilde{p}_3 & -\tilde{p}_0^2+\tilde{p}_1^2+\tilde{p}_2^2-\tilde{p}_3^2 \end{pmatrix} \tag{6.4}$$

with $\quad D = \tilde{p}_0^2+\tilde{p}_1^2+\tilde{p}_2^2+\tilde{p}_3^2$

is a special orthogonal matrix, and it satisfies the condition (6.2). In fact, the point $U(t)\ (0\ 0\ 1)^\top$ on the unit sphere is exactly the image of $\tilde{\mathbf{p}}(t)$ under the generalized stereographic projection δ, cf. (2.4). Thus, the motion (6.1) with $U(t) = U_0(t)$ is a frame of the PH curve $\mathbf{x}(t)$. □

This proof is based on the classical representation of a rotation matrix with the help of its so–called *Euler parameters*, see [2]. The Euler parameters of a rotation matrix are related to the unit quaternion which describes the rotation U. There exist a close relationship between the Euler parameters and the generalized stereographic projection, see [8, 17].

The definition of the frame of a space curve leaves one degree of freedom, as it is possible to rotate the frame around the tangent. For instance, any spatial motion

$$(\mathbf{q}, t) \mapsto \mathbf{q}'(t) = \mathbf{x}(t) + U_0(t)\, Z_0(t)\, \mathbf{q} \tag{6.5}$$

with $U_0(t)$ as defined in (6.4) and

$$Z_0(t) = \frac{1}{\xi^2 + \eta^2} \begin{pmatrix} \xi^2 - \eta^2 & -2\,\xi\,\eta & 0 \\ 2\,\xi\,\eta & \xi^2 - \eta^2 & 0 \\ 0 & 0 & \xi^2 + \eta^2 \end{pmatrix} \tag{6.6}$$

for arbitrary polynomials $\xi(t)$, $\eta(t)$ (which should not have any joint roots) is a rational frame of the PH curve $\mathbf{x}(t)$, see Lemma 1.

For the construction of sweeping surfaces using frames it is advantageous to use the frame which rotates as little as possible. This frame is called the *rotation minimizing frame* of the given curve, see [11, 15, 18]. For this frame, the angular velocity is as small as possible. It leads to good shapes of the generated sweeping surfaces.

The forthcoming conference article [9] gives a kinematical discussion of rotation minimizing frames. For curves whose unit tangents form a circular arc, the associated rotation minimizing frame is computed exactly. For instance, this is automatically true for PH space cubics. In addition, based on quaternion calculus, the article derives a scheme for constructing rational approximations of rotation minimizing frames. Due to space limitations we cannot present more details. The interested reader should consult [9]. Recently, Mäurer [13] has independently discussed rational approximations to the RMF.

An example is depicted in Figure 6. The left figure shows a cubic PH spline curve with three segments (black curve). This curve has been obtained by converting the thick grey curve into a PH spline curve, as described in the previous section. The dashed lines are the tangents at the segment end points of the PH spline. There is virtually no difference between the original curve and the approximating PH cubic spline curve.

A sweeping surface which has been generated by a rational approximation of the rotation minimizing frame is shown on the right–hand side. The cubic PH spline curve serves as the spine curve of the sweeping surface.

7 Concluding remarks

In this paper we have presented a general approach to the construction of Pythagorean hodograph space curves. In the case of PH cubics, we were able to discuss the existence of real solutions to Hermite interpolation of

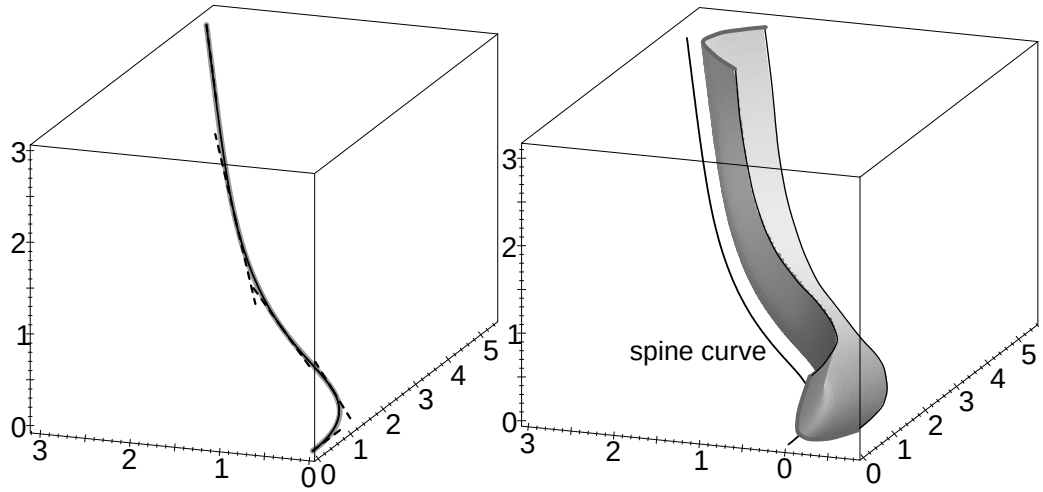

(a) (b)

FIGURE 6. Rational PH spline curve (a) and a sweeping surface (b) which is generated by a rational approximation of the rotation minimizing frame

G^1 boundary data. The results can be used for converting given space curve into cubic PH splines. As a matter of future research, we will try to give a similar discussion for Hermite interpolation of G^2 boundary data with PH quintics.

The second part of the paper was devoted to rational frames of PH curves. Using the close connection between rational hodographs (which are rational spherical curves) and Euler parameters of orthogonal matrices, a general representation of the rational frames has been presented. By combining this representation with the above conversion procedure, it is possible to construct rational approximations to the so–called rotation minimizing frame of a space curve.

References

[1] G. Albrecht, R.T. Farouki, Construction of C^2 Pythagorean-hodograph interpolating splines by the homotopy method, *Adv. Comput. Math.*, **5**, 417-442, 1996.

[2] O. Bottema, B. Roth, *Theoretical Kinematics*, North–Holland, Amsterdam, 1979.

[3] R. Dietz, J. Hoschek, B. Jüttler, An algebraic approach to curves and surfaces on the sphere and on other quadrics, *Comput. Aided Geom. Design*, **10**, 211-229, 1993.

[4] R.T. Farouki, C.A. Neff, Hermite interpolation by Pythagorean hodograph quintics, *Math. Comput.*, **64**, 1589-1609, 1995.

[5] R.T. Farouki, T. Sakkalis, Pythagorean-hodograph space curves, *Adv. Comput. Math.*, **2**, 41-66, 1994.

[6] R. Goldman, T. Sederberg, D. Anderson, Vector Elimination: A technique for the implicitization, inversion and intersection of planar parametric rational polynomial curves, *Comput. Aided Geom. Design*, **1**, 327–356, 1984.

[7] J. Hoschek, D. Lasser, *Fundamentals of Computer Aided Geometric Design,* AK Peters, Wellesley MA, 1993.

[8] B. Jüttler, Über zwangläufige rationale Bewegungsvorgänge. *Sitzungsber., Abt. II, Österr. Akad. Wiss., Math.-Naturwiss. Kl.*, **202**, 117-132, 1993.

[9] B. Jüttler, Rotation minimizing spherical motions, submitted to the Proceedings of ARK'98, Kluwer Academic Publishers, 1998.

[10] B. Jüttler, M.G. Wagner, Computer Aided Design with Spatial Rational B–Spline Motions, *ASME J. of Mech. Design*, **118**, 193–201, 1996.

[11] F. Klok, Two moving coordinate frames for sweeping along a 3D trajectory, *Comput. Aided Geom. Design*, **3**, 217-229, 1986.

[12] E. Kreyszig, *Differential geometry,* Oxford University Press, London, 1964.

[13] C. Mäurer, Spine curve oriented surface design using cubic PH space curves, manuscript, NTU Athens, 1998.

[14] D. Pedoe, *A Course of Geometry for Colleges and Universities,* University Press, Cambridge 1970.

[15] H. Pottmann, M. Wagner, Contributions to Motion Based Surface Design, manuscript, 1998.

[16] M. Wagner, B. Ravani, Curves with Rational Frenet–Serret motion, *Comput. Aided Geom. Design*, **15**, 79–101, 1997.

[17] J. Wallner, H. Pottmann, Rational blending surfaces between quadrics, *Comput. Aided Geom. Design*, **14**, 407–419, 1997.

[18] W. Wang, B. Joe, Robust computation of the rotation minimizing frame for sweep surface modeling, *Comput.–Aided Design*, **29**, 379–391, 1997.